KEY POINTS

- No mouse model completely simulates the entire process of plaque rupture, including the development of vulnerable plaques with large necrotic cores and thin fibrous caps, the disruption of fibrous caps and spontaneous thrombotic occlusion.

- Coronary imaging modalities identified the presence of plaque ruptures without thrombotic occlusion causing myocardial infarction.

- The brachiocephalic artery in ApoE-deficient mice fed an HFD with or without angiotensin II infusion is a feasible model of plaque rupture presenting multiple buried fibrous caps indicating previous plaque ruptures.

of appropriate animal models of plaque rupture. In this review, we summarize the current concept of vulnerable plaques and plaque rupture in clinical and pathological studies and the recent development and use of mouse models for the study of plaque rupture.

WHAT DO HUMAN STUDIES TELL US ABOUT PLAQUE RUPTURE AND VULNERABLE PLAQUES?

In postmortem pathological studies in cases of sudden coronary death, plaque rupture is defined as a fibroatheroma with cap disruption, in which a luminal thrombus communicates with the underlying necrotic core [1,2]. Plaque ruptures were found in 60% of the cases, suggesting that plaque rupture and subsequent thrombotic occlusion are a central mechanism of AMI resulting in sudden death [1]. A ruptured lesion typically has a large necrotic core and a disrupted fibrous cap infiltrated by macrophages and lymphocytes. The smooth muscle cell content within the fibrous cap at the rupture site is frequently sparse. These observations characterized the concept of a 'vulnerable plaque' or TCFA, which is prone to plaque rupture, causing AMI [2]. This concept largely depends on postmortem pathological studies, which are essentially retrospective and are affected by selection biases and often lack the assessment of background pathophysiology and medical treatments before coronary death.

In clinical settings, IVUS has been used to determine vessel geometry including vessel area and plaque area during coronary interventions, and it can also detect ruptured plaques that contain a cavity that communicates with the lumen with an overlying residual fibrous cap fragment [4]. Ruptured plaques have been observed using IVUS in 49% of 122 AMI patients and 25% of 113 stable

angina patients. IVUS can also detect hypoechoic plaques with deep ultrasound attenuation (attenuated plaque) that may correspond to a high lipid content in the plaque, which is more often observed in patients with acute coronary syndrome (ACS) than in those with stable angina [1,5].

More recently, OCT was introduced as another modality for intracoronary imaging, using near-infrared light with a shorter wavelength and higher frequency than ultrasound. OCT possesses higher spatial resolution (10–20 μm) compared with IVUS (100–200 μm), which enables cardiologists to detect fibrous cap disruption with better sensitivity than IVUS and to determine fibrous cap thickness in vivo [2,3•]. Kubo et al. [5] have shown that OCT often demonstrates thin fibrous caps on attenuated plaques identified by IVUS, which may also correspond to TCFAs or vulnerable plaques defined by pathological studies [3•]. One prospective study using IVUS [1,2,6] has demonstrated that TCFAs determined on the basis of radiofrequency IVUS are indeed a risk factor for coronary events in non-culprit coronary lesions after successful coronary interventions, supporting the concept of rupture-prone vulnerable plaques. OCT has also been reported to detect plaque ruptures in 73% of 30 AMI cases and is significantly more sensitive than IVUS, which detected plaque rupture in 40% of the same population [1,5]. Notably, the use of intra-vascular imaging has revealed the presence of asymptomatic plaque ruptures in patients with stable coronary artery disease without AMI [2,3•], which might result in the buried fibrous caps (multiple ruptures) found in cases of sudden coronary death [1,4].

Human studies tell us that thrombotic occlusion of the ruptured coronary plaques is the main culprit for AMI in cases of coronary death and nonfatal myocardial infarction, and that asymptomatic plaque ruptures are frequently observed even in the nonculprit coronary arteries. Therefore, the burden of vulnerable plaques and silent plaque ruptures may predispose stable patients to ACS including AMI via thrombus formation in the coronary lumen.

WHICH PATHOPHYSIOLOGY SHOULD BE MODELLED?

Pathophysiological process of plaque rupture leading to AMI could be divided into three steps: plaque destabilization, namely fibrous cap thinning over large necrotic core and macrophage infiltration, plaque rupture, a disruption of the fibrous caps, and thrombotic occlusion of the artery. To develop an animal model for plaque rupture that is appropriate and useful, the ideal model should simulate

the complete process of plaque destabilization and rupture, and spontaneous thrombosis that results in arterial occlusion. Another more practical concept based on the fact that not every plaque rupture causes thrombotic occlusion leading to a clinical event [5,6] is that the model should be used for the quantitative analysis of each process of plaque destabilization (formation of a TCFA or vulnerable plaque) and rupture, to evaluate the effects of concomitant factors or novel therapeutic approaches.

MOUSE MODELS OF PLAQUE RUPTURE IN THE BRACHIOCEPHALIC ARTERY

Hypercholesterolaemic animals have been used for studies on atherosclerosis, including the Watanabe heritable hyperlipidaemic rabbit, which has a low-density lipoprotein receptor (LDLR) gene defect analogous to familial hypercholesterolaemia in humans [7], LDLR-deficient mice [8] and apolipoprotein E (ApoE)-deficient mice [9]. Earlier studies have used these animal models to analyse the mechanisms of general atherosclerosis in the aorta or aortic roots; however, the investigation of aortic atherosclerosis in animals may not necessarily reveal the mechanistic link to plaque destabilization and rupture because aortic atherosclerotic lesions in many animal models do not spontaneously progress to plaque rupture. In 1994, Nakashima *et al.* [10] reported that older ApoE-deficient mice fed a high-fat diet (HFD) develop several forms of advanced lesions in branches of the aorta.

More recently, Johnson *et al.* [11,12] have identified the brachiocephalic/innominate artery as the best susceptible site for atherosclerosis in ApoE-deficient mice fed an HFD, in which lesions represent several key histological features of ruptured human plaques, including the spontaneous disruption of fibrous caps with evidence of intraplaque haemorrhage, the infiltration of inflammatory cells and the presence of large necrotic cores and thin fibrous caps. In this model, acute plaque rupture is defined as a visible defect in the fibrous cap that is accompanied by intrusion of erythrocytes into the plaque. Buried fibrous caps are defined as elastin layers overlain with foam cells, which suggest previous plaque ruptures [11,12]. Using this model, it was feasible to examine the therapeutic effects of a statin, which reduced the incidence of buried fibrous caps, plaque size and plaque lipid content (necrotic core) over 8 weeks of plaque rupture induction and statin treatment [12].

Changes in fluid shear stress may be possible mechanisms by which atherosclerotic plaques are frequently observed in the branching points of the arteries [13]. Cheng *et al.* [14] developed a perivascular shear stress modifier that induces regions of lowered, increased and lowered/oscillatory shear stress in mouse carotid arteries and studied plaque formation and composition. Lower shear stress was associated with vulnerable plaque phenotype (fewer smooth muscle cells, less collagen and more lipids), and higher expression of inflammatory cytokines and matrix metalloproteinase (MMP) activity, although plaque rupture or disruption of fibrous caps was not observed [14]. This study not only implies that the changes in shear stress may contribute to the regional preference of plaque destabilization, including the curved coronary arteries in humans and the brachiocephalic arteries in mice, but also suggests that yet unidentified factors might be required for plaque rupture or fibrous cap disruption in the cast-placed carotid arteries.

GENES AFFECTING PLAQUE RUPTURE IN APOLIPOPROTEIN E DEFICIENT MICE

The brachiocephalic artery of ApoE-deficient mice is a good subject to analyse the role of the molecules of interest in plaque destabilization and rupture using genetically engineered mice. MMPs are found in human atherosclerotic plaques and suggested to play a causative role in matrix degradation during plaque destabilization [15]. Gough *et al.* [16] generated haematopoietic stem cells transfected with macrophage-specific retrovirus encoding active form of MMP-9, which was transferred into irradiated recipient ApoE-deficient mice fed a normal chow diet. Induction of active MMP-9 was found in macrophages in the atherosclerotic lesions and resulted in enhanced elastin degradation and disruption of fibrous caps with intraplaque haemorrhage in the brachiocephalic arteries, confirming the causative role of MMP-9 in plaque destabilization and rupture.

Serine protease urokinase plasminogen activator (uPA) catalyzes and activates MMP precursors. Hu *et al.* [17] tested their hypothesis that overexpression of uPA in macrophage may enhance plaque destabilization and rupture in ApoE-deficient mice with uPA overexpression in macrophages by bone marrow transfer. Macrophages in the plaques expressed uPA and the aortic conditioned medium showed higher MMPs activity. Plaques in the brachiocephalic artery showed higher incidence of fibrous cap disruption, although the difference was not statistically significant [17].

Another study by van Herck *et al.* [18] employed fibrillin-1 C1039G mutant mice crossed with ApoE-deficient mice, which caused spontaneous fragmentation of elastin fibres in the arterial walls.

Atherosclerotic plaques in the proximal ascending aorta and the brachiocephalic artery in fibrillin-1 mutant mice indeed contained the increased number of buried fibrous caps. Interestingly, fibrillin-1 mutant is associated with increased plaque area, macrophage infiltration and smooth muscle apoptosis as markers of plaque destabilization, which suggested the role of arterial composition and stiffness in plaque destabilization [18]. These studies support the concept of MMP-dependent degradation of fibrous cap components as a central mechanism of plaque rupture, and also suggest the presence of vicious cycle among the elastin degradation, plaque rupture and plaque destabilization.

ANGIOTENSIN II ACCELERATES PLAQUE DESTABILIZATION IN THE MOUSE MODEL

One weakness of this plaque rupture model in the brachiocephalic arteries of ApoE-deficient mice is that plaque rupture (acute plaque rupture and buried fibrous caps) is too infrequent (10–20% without HFD feeding [16] and 40–60% per plaque after HFD feeding). In one study [12], an excess of 60 ApoE-deficient mice fed an HFD was needed per group to ensure that the study was adequately powered to analyse the therapeutic effects of an antiatherosclerotic drug.

To overcome this problem, our group chronically infused angiotensin II in addition to feeding ApoE-deficient mice an HFD [19■■]. Angiotensin II has been suggested to affect several mechanisms that accelerate atherogenesis, including blood pressure elevation, monocyte recruitment, macrophage activation and increased oxidative stress. Indeed, we and other researchers [20–23] have shown that angiotensin II accelerates aortic atherosclerosis and abdominal aneurysm formation after a 4-week continuous infusion in ApoE-deficient mice. In our recent study [19■■], ApoE-deficient mice were fed an HFD containing 21% fat from lard and supplemented with 0.15% (wt/wt) pure cholesterol starting at 18 weeks of age. After 4 weeks on the HFD, mice were administered an angiotensin II infusion (1.9 mg/kg per day) for 4 weeks. The brachiocephalic

arteries were stained with haematoxylin-eosin (HE) or Elastica van Gieson (EVG) to determine the incidence of the disruption of fibrous caps and buried fibrous caps, the fibrous cap thickness and the lipid core area [19■■].

In this modified mouse model, chronic angiotensin II infusion increased the incidence of buried fibrous caps from 1.60 ± 0.22 ruptures per animal to 3.33 ± 0.20 per animal ($P < 0.0001$), with decreased fibrous cap thickness, and increased the plaque area and the size of the necrotic core (Table 1, Fig. 1). Using this modified mouse model for plaque rupture, we have shown that the addition of cholesterol oxidation products to the diet accelerated plaque destabilization (fibrous cap thinning and macrophage infiltration), enhanced MMP activity in the plaque and increased the incidence of plaque rupture through the recruitment of CCR2+Ly6C^high inflammatory monocytes, which is blunted by CCR2 deficiency. Furthermore, the cholesterol absorption inhibitor ezetimibe decreased plasma lipid levels and prevented the acceleration of plaque destabilization and rupture induced by dietary oxysterol and was associated with the reduction of inflammatory monocytes in the peripheral blood [19■■]. This mouse model was useful for highlighting the role of inflammatory monocytes and the importance of lipid-lowering therapy during plaque destabilization and rupture with an acceptable sample size and experimental duration.

THROMBOSIS IN THE ARTERIES OF APOLIPOPROTEIN E DEFICIENT MICE

The mouse model of plaque rupture in the brachiocephalic arteries of ApoE-deficient mice, however, has been criticised due to dissimilarities in lesion morphology compared with vulnerable plaques in humans, one of which is that occlusive thrombosis is extremely rare in the mouse brachiocephalic arteries [12,24–26]. The absence of thrombotic occlusion after the disruption of fibrous caps is thought to be a reflection of differences in the coagulation and thrombolytic systems between mice and humans, as the plasma level of

Table 1. Effects of high-fat diet and angiotensin II infusion on plaque phenotype

Group	Group size, n	Acute plaque rupture, n	Buried fibrous caps per animal, n	Fibrous cap thickness, μm	Plaque area, $\times 10^3 \mu m^2$	Plaque necrotic core, %
HFD	10	0	1.60 ± 0.22	2.98 ± 0.27	125.3 ± 12.5	9.4 ± 0.9
HFD and angiotensin II	21	3	$3.33 \pm 0.20^*$	$1.30 \pm 0.09^*$	$174.8 \pm 13.0^*$	$15.0 \pm 1.7^*$

ApoE-deficient mice (18-week-old) were fed high-fat diet (HFD) for 8 weeks. After 4 weeks on HFD, mice received angiotensin II infusion (1.9 mg/kg per day) for 4 weeks. This table is an original unpublished observation by the authors.
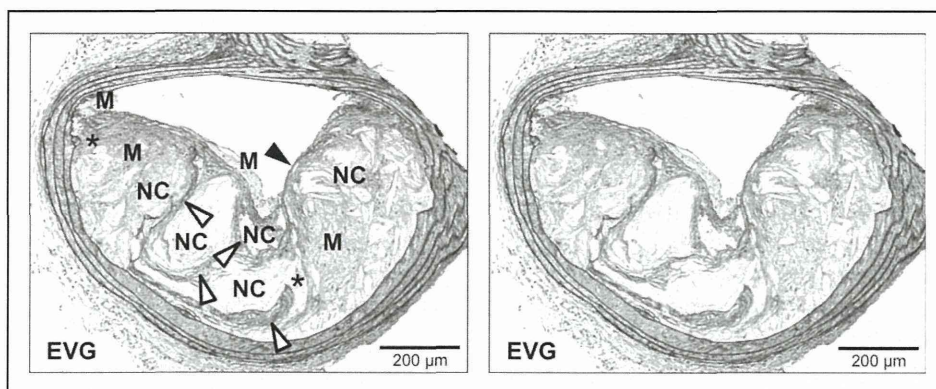*$P < 0.05$ vs. HFD group.

FIGURE 1. Histology of the brachiocephalic artery of an apoliprotein E deficient mouse fed a high-fat diet and infused with angiotensin II. The artery was stained with Elastica van Gieson (EVG), with (left) or without (right) captions. Asterisks (∗) indicate disrupted fibrous caps overlain with macrophages or a necrotic core. White triangles indicate buried fibrous caps, whereas the black triangle indicates the thinnest segment of the fibrous cap over the necrotic core. M, macrophage; NC, necrotic core. This figure is an original unpublished observation by the authors.

plasminogen activator inhibitor (PAI)-1 is lower in mice than in humans, whereas the fibrinogen and tissue-type plasminogen activator (tPA) concentrations are similar [27].

A recent publication by Aono *et al.* [28] used a mouse model of plaque rupture that is accompanied by thrombosis. This model was first introduced by Sasaki *et al.* [29], and it employs two interventions, the ligation of the common carotid artery, which ceases blood flow and causes intimal hyperplasia, and cuff placement proximal to the ligation site to induce disruption of the neointima and thrombus formation in ApoE-deficient mice fed a normal diet. Another study by Jin *et al.* [30▪▪] introduced a new model of plaque rupture with thrombus formation in the common carotid arteries of ApoE-deficient mice fed a normal diet. This model employs two different interventions: the ligation of both the internal and external carotid arteries, which modifies shear stress, and the induction of renovascular hypertension by a partial ligation of a unilateral renal artery, which activates the endogenous renin-angiotensin system. Eight weeks after the ligations, the common carotid arteries displayed increased neointima, decreased smooth muscle content and increased macrophage infiltration, and 50% of the arteries also contained a thrombus. These models [28,29,30▪▪] succeeded in thrombus formation over the disrupted neointima. However, the absence of a necrotic core in the lesions and the artificial limitation of the blood flow prior to the thrombus formation makes it difficult to interpret the findings to guide further research on the mechanisms of spontaneous plaque rupture in humans using these models [25,31]. A recent study by von Elverfeldt *et al.* [32] employed magnetic resonance contrast conjugated with an antibody for glycoprotein IIb/IIIa-receptor targeting active platelets. MRI detected activated platelets on mechanically ruptured (by a needle) atherosclerotic plaques in the external carotid arteries of ApoE-deficient mice *in vivo*, with a high sensitivity detecting thrombus occupying only 2% of the vascular lumen [32]. This technique may be applicable for spontaneous thrombus formation if any after plaque ruptures in the brachiocephalic arteries of mice, which may be otherwise undetectable after fibrinolysis [27].

PLAQUE COMPOSITION AND BIOMECHANICS IN HUMAN AND MOUSE PLAQUES

Another dissimilarity between human and mouse plaques is the composition and resulting mechanical stress from the luminal pressure on the plaques. Ohayon *et al.* [33▪] simulated mechanical stress and strain distribution in aortic atherosclerotic lesions from ApoE-deficient mice on the basis of the plaque component stiffness, in which the plaque components were classified as a lipid-rich region, a hypocellular fibrosis region and a cellular fibrosis region. They found that the differences in the mechanical properties of plaque components between mice and humans affect the amplitude and spatial distribution of the simulated intraplaque stress, and the estimated in-vivo intraplaque stress was 20-fold less in the mouse aorta [33▪]. Campbell *et al.* [34▪] also compared the morphology and biomechanics of mouse models in the brachiocephalic arteries with TCFAs in human coronary arteries using another computational model. In three mouse

models including ApoE-deficient and LDLR-deficient mice both fed an HFD for 8 weeks with simultaneous infusion of angiotensin II and ApoE-deficient mice fed a regular chow diet for 1 year, there were significant morphological differences compared with human TCFA plaques, including the plaque burden, plaque thickness, eccentricity and amount of the vessel wall covered by a lesion as well as significant differences in the relative composition of the plaques. On the basis of computational modelling of the relative stress distribution on the walls [35] of murine and human plaques, Campbell *et al.* [34■] suggested that although human TCFA plaques have the highest stresses in the thin fibrous cap, murine lesions do not have such stress distributions. Instead, the maximum amounts of local stress were placed on the media and adventitia, away from the plaque [34■].

These studies indicate important aspects for further analysing the mechanism of plaque rupture in humans and mice and the difference in the incidence of plaque rupture in these two species. However, because the morphology and composition are quite diverse in ruptured plaques in humans, and because the computational simulations of intraplaque stress include several assumptions without validation by direct measurement, these mechanical differences may not directly affect the importance and the usefulness of mouse models of plaque rupture.

CONCLUSION

No mouse model examined herein completely simulates the entire process of plaque rupture, including the development of vulnerable plaques with large necrotic cores and thin fibrous caps, the disruption of fibrous caps (plaque rupture) and spontaneous thrombotic occlusion. However, in practice, the brachiocephalic artery in ApoE-deficient mice fed an HFD with or without angiotensin II infusion is a feasible model for plaque rupture. This model enables researchers to analyse the role of pathophysiological and genetic factors that accelerate plaque destabilization and rupture, and qualitatively and quantitatively examine the effects of experimental therapies. Further development may allow the modelling of spontaneous thrombotic occlusion of the arteries.

Acknowledgements

Conflicts of interest

There are no conflicts of interest.

REFERENCES AND RECOMMENDED READING

Papers of particular interest, published within the annual period of review, have been highlighted as:
■ of special interest
■■ of outstanding interest
Additional references related to this topic can also be found in the Current World Literature section in this issue (p. 446).

1. Virmani R, Kolodgie FD, Burke AP, *et al.* Lessons from sudden coronary death: a comprehensive morphological classification scheme for atherosclerotic lesions. Arterioscler Thromb Vasc Biol 2000; 20:1262–1275.
2. Finn AV, Nakano M, Narula J, *et al.* Concept of vulnerable/unstable plaque. Arterioscler Thromb Vasc Biol 2010; 30:1282–1292.
3. Gutierrez-Chico JL, Alegria-Barrero E, Teijeiro-Mestre R, *et al.* Optical
■ coherence tomography: from research to practice. Eur Heart J Cardiovasc Imag 2012; 13:370–384.
This review summarizes optical coherence tomographic findings including plaque rupture, intracoronary thrombosis and TCFA in cases of ACS. The findings support the causative role of TCFA in ACS and also document the presence of silent plaque ruptures in stable coronary artery disease cases.
4. Hong M-K, Mintz GS, Lee CW, *et al.* Comparison of coronary plaque rupture between stable angina and acute myocardial infarction: a three-vessel intravascular ultrasound study in 235 patients. Circulation 2004; 110: 928–933.
5. Kubo T, Matsuo Y, Ino Y, *et al.* Optical coherence tomography analysis of attenuated plaques detected by intravascular ultrasound in patients with acute coronary syndromes. Cardiol Res Pract 2011; 2011: 687515.
6. Stone GW, Maehara A, Lansky AJ, *et al.* A prospective natural-history study of coronary atherosclerosis. N Engl J Med 2011; 364:226–235.
7. Kita T, Brown MS, Watanabe Y, Goldstein JL. Deficiency of low density lipoprotein receptors in liver and adrenal gland of the WHHL rabbit, an animal model of familial hypercholesterolemia. Proc Natl Acad Sci U S A 1981; 78:2268–2272.
8. Ishibashi S, Brown MS, Goldstein JL, *et al.* Hypercholesterolemia in low density lipoprotein receptor knockout mice and its reversal by adenovirus-mediated gene delivery. J Clin Invest 1993; 92:883–893.
9. Maeda N. Development of apolipoprotein E-deficient mice. Arterioscler Thromb Vasc Biol 2011; 31:1957–1962.
10. Nakashima Y, Plump AS, Raines EW, *et al.* ApoE-deficient mice develop lesions of all phases of atherosclerosis throughout the arterial tree. Arterioscler Thromb 1994; 14:133–140.
11. Johnson JL, Jackson CL. Atherosclerotic plaque rupture in the apolipoprotein E knockout mouse. Atherosclerosis 2001; 154:399–406.
12. Johnson J, Carson K, Williams H, *et al.* Plaque rupture after short periods of fat feeding in the apolipoprotein E-knockout mouse: model characterization and effects of pravastatin treatment. Circulation 2005; 111:1422–1430.
13. Traub O, Berk BC. Laminar shear stress: mechanisms by which endothelial cells transduce an atheroprotective force. Arterioscler Thromb Vasc Biol 1998; 18:677–685.
14. Cheng C, Tempel D, van Haperen R, *et al.* Atherosclerotic lesion size and vulnerability are determined by patterns of fluid shear stress. Circulation 2006; 113:2744–2753.
15. Galis ZS, Sukhova GK, Lark MW, Libby P. Increased expression of matrix metalloproteinases and matrix degrading activity in vulnerable regions of human atherosclerotic plaques. J Clin Invest 1994; 94:2493–2503.
16. Gough PJ, Gomez IG, Wille PT, Raines EW. Macrophage expression of active MMP-9 induces acute plaque disruption in apoE-deficient mice. J Clin Invest 2006; 116:59–69.
17. Hu JH, Du L, Chu T, *et al.* Overexpression of urokinase by plaque macrophages causes histological features of plaque rupture and increases vascular matrix metalloproteinase activity in aged apolipoprotein e-null mice. Circulation 2010; 121:1637–1644.
18. van Herck JL, De Meyer GRY, Martinet W, *et al.* Impaired fibrillin-1 function promotes features of plaque instability in apolipoprotein E-deficient mice. Circulation 2009; 120:2478–2487.
19. Sato K, Nakano K, Katsuki S, *et al.* Dietary cholesterol oxidation products
■■ accelerate plaque destabilization and rupture associated with monocyte infiltration/activation via the MCP-1-CCR2 pathway in mouse brachiocephalic arteries: therapeutic effects of ezetimibe. J Atheroscler Thromb 2012; 19: 986–998.
This study shows a good example for the use of a model of plaque rupture in the brachiocephalic artery of ApoE-deficient mice to examine the role of monocyte-mediated inflammation and the effects of an experimental treatment for plaque destabilization and rupture.

20. Daugherty A, Manning MW, Cassis LA. Angiotensin II promotes atherosclerotic lesions and aneurysms in apolipoprotein E-deficient mice. J Clin Invest 2000; 105:1605–1612.
21. Ni W, Kitamoto S, Ishibashi M, *et al.* Monocyte chemoattractant protein-1 is an essential inflammatory mediator in angiotensin II-induced progression of established atherosclerosis in hypercholesterolemic mice. Arterioscler Thromb Vasc Biol 2004; 24:534–539.
22. Ishibashi M, Egashira K, Zhao Q, *et al.* Bone marrow-derived monocyte chemoattractant protein-1 receptor CCR2 is critical in angiotensin II-induced acceleration of atherosclerosis and aneurysm formation in hypercholesterolemic mice. Arterioscler Thromb Vasc Biol 2004; 24: e174–e178.
23. Satoh K, Nigro P, Matoba T, *et al.* Cyclophilin A enhances vascular oxidative stress and the development of angiotensin II-induced aortic aneurysms. Nat Med 2009; 15:649–656.
24. Rosenfeld ME, Polinsky P, Virmani R, *et al.* Advanced atherosclerotic lesions in the innominate artery of the ApoE knockout mouse. Arterioscler Thromb Vasc Biol 2000; 20:2587–2592.
25. Schwartz SM, Galis ZS, Rosenfeld ME, Falk E. Plaque rupture in humans and mice. Arterioscler Thromb Vasc Biol 2007; 27:705–713.
26. Bentzon JF, Falk E. Atherosclerotic lesions in mouse and man: is it the same disease? Curr Opin Lipidol 2010; 21:434–440.
27. Tsakiris DA, Scudder L, Hodivala-Dilke K, *et al.* Hemostasis in the mouse (Mus musculus): a review. Thromb Haemost 1999; 81:177–188.
28. Aono J, Suzuki J, Iwai M, *et al.* Deletion of the angiotensin II type 1a receptor prevents atherosclerotic plaque rupture in apolipoprotein E-/- mice. Arterioscler Thromb Vasc Biol 2012; 32:1453–1459.
29. Sasaki T, Kuzuya M, Nakamura K, *et al.* A simple method of plaque rupture induction in apolipoprotein E-deficient mice. Arterioscler Thromb Vasc Biol 2006; 26:1304–1309.
30. Jin S-X, Shen L-H, Nie P, *et al.* Endogenous renovascular hypertension
■■ combined with low shear stress induces plaque rupture in apolipoprotein E-deficient mice. Arterioscler Thromb Vasc Biol 2012; 32:2372–2379.
This study introduced a new mouse model of plaque rupture with a thrombosis in ApoE-deficient mice, although the use of two interventions adds some difficulties for the interpretations.
31. Falk E, Schwartz SM, Galis ZS, Rosenfeld ME. Neointimal cracks (plaque rupture?) and thrombosis in wrapped arteries without flow. Arterioscler Thromb Vasc Biol 2007; 27:248–249; author reply 250–252.
32. von Elverfeldt D, von Muhlen C, Wiens K, *et al.* In vivo detection of activated platelets allows characterizing rupture of atherosclerotic plaques with molecular magnetic resonance imaging in mice [Internet]. PLoS ONE 2012; 7:e45008.
33. Ohayon J, Mesnier N, Broisat A, *et al.* Elucidating atherosclerotic vulnerable
■ plaque rupture by modeling cross substitution of ApoE-/- mouse and human plaque components stiffnesses. Biomech Model Mechanobiol 2012; 11:801–813.
This study used a computational model to reconstruct in vivo stress/strain distribution in atherosclerotic plaques in mice and humans, based on the measured stiffness of plaque tissue composition. Calculated peak stress on the fibrous cap was higher in humans than in mice.
34. Campbell IC, Weiss D, Suever JD, *et al.* Biomechanical modeling and morpho-
■ logy analysis indicates plaque rupture due to mechanical failure unlikely in atherosclerosis-prone mice. AJP Heart Circ Physiol 2013; 304:H473–H486.
This article, together with reference [33■], showed that computational modelling of the plaque pathological morphology may suggest the biomechanical difference between mouse and human, although further validation of the modelling is required.
35. Hallow KM, Taylor WR, Rachev A, Vito RP. Markers of inflammation collocate with increased wall stress in human coronary arterial plaque [Internet]. Biomech Model Mechanobiol 2009; 8:473–486.

Reviews

Nanoparticle-Mediated Drug Delivery System for Cardiovascular Disease

Tetsuya Matoba,[1] MD *and* Kensuke Egashira,[1,2] MD

Summary

Administration of drugs and other therapeutic agents has been the central strategy of contemporary medicine for cardiovascular disease. The use of a drug delivery system (DDS) is always demanded to enhance the efficacy and safety of therapeutic agents, and improve the signal-to-noise ratio of imaging agents. Nano-scale materials modify in vivo drug kinetics, depending on (patho)physiological mechanisms such as vascular permeability and incorporation by the mononuclear phagocyte system, which constitute 'passive-targeting' properties of nano-DDS. By contrast, an 'active-targeting' strategy employs a specific targeting structure on nano-DDS, which binds to the target molecule that is specific for a certain disease process, such as tumor specific antigens and the induction of adhesion molecules. In this review, we summarize recent studies that applied nano-DDS for the diagnosis and treatment of cardiovascular disease, especially focusing on atherosclerosis and myocardial ischemia-reperfusion (IR) injury. Pathophysiological changes in atherosclerosis and myocardial IR injury are successfully targeted by nano-DDS and preclinical studies in animals showed positive effects of nano-DDS enhancing efficacy and reducing adverse effects. The development of nano-DDS in clinical medicine is keenly being awaited. (Int Heart J 2014; 55: 281-286)

Key words: Nanotechnology, Atherosclerosis, Myocardial infarction, Ischemia reperfusion, Inflammation

Nanoparticle-Mediated Drug Delivery Systems

Administration of drugs and other therapeutic agents has been the central strategy of contemporary medicine, based on the concept that a certain disease is caused by a formation of abnormal or diseased cells within healthy organs and the body. In order for drugs to affect disregulated organs and cells, drugs need to overcome physiological barriers, namely circulation to organs, and tissue to cells, and reach target molecules within the cells. On the other hand, all drugs possess potential toxicity that may limit their safe dose and thereby therapeutic efficacy. Targeting drugs to diseased organs/cells may reduce the potential risks of adverse effects; therefore, the use of a drug delivery system (DDS) is always needed to enhance the efficacy and safety of therapeutic agents, and overcome any drawbacks of the agents, such as toxicity, low water solubility, poor bioavailability, and low organ specificity. Moreover, targeting delivery is a desirable property for diagnostic purposes as it improves the signal-to-noise ratio and optimizes sensitivity and specificity.

Recent application of nanotechnology to medicine has developed nanoparticle-mediated DDS (nano-DDS), which modifies the in vivo kinetics of therapeutic and diagnostic agents. One of the most important motives for nano-DDS is drug targeting, which may utilize physiology and pathophysiological properties unique to certain disease processes.[1,2] Nano-

DDS can be composed of a variety of materials and structures, including lipids to form micelles or liposomes,[3,4] polymers,[5-7] dendrimers,[8] carbon nanotubes, and metallic nanoparticles such as crystalline iron oxide and gold nanoparticles (Figure 1).[9] Here we describe selected examples of nano-scale materials tested as nano-DDS. Micelles are formed from lipids and other amphiphilic artificial molecules such as polymers.[10] Micelles self-assemble in aqueous solution and may incorporate hydrophobic therapeutic agents to overcome solubility problems. The size (usually 10-100 nm in diameter) and the enclosed space are more confined to those of liposomes (Figure 1A). Liposomes mainly consist of phospholipids that form bilayers with an aqueous phase inside, and are heterogeneous in size, often ranging from a few hundreds to thousands of nanometers in diameter. Liposomes are the most extensively tested nano-DDS in basic and clinical medicine with United States Food and Drug Administration (FDA) approval. Chemicals, nucleotides, and also crystalline metals are incorporated in liposomes (Figure 1B).[3,4] Currently, two polymers, polylactide (PLA) and poly(lactide-co-glycolide) (PLGA), are used for the synthesis of FDA-approved polymeric biodegradable nano-DDS.[2] PLGA polymers may incorporate hydrophilic and hydrophobic therapeutic agents including chemicals and nucleotides by emulsion solvent diffusion methods, and are being tested for intractable diseases including cardiovascular disease (Figure 1C).[11-20] Dendrimers are highly branched macromole-

A   B   C

Micelle   Liposome   Polymeric
                             nanosphere

D   E   F

Dendrimer   Carbon   Metallic
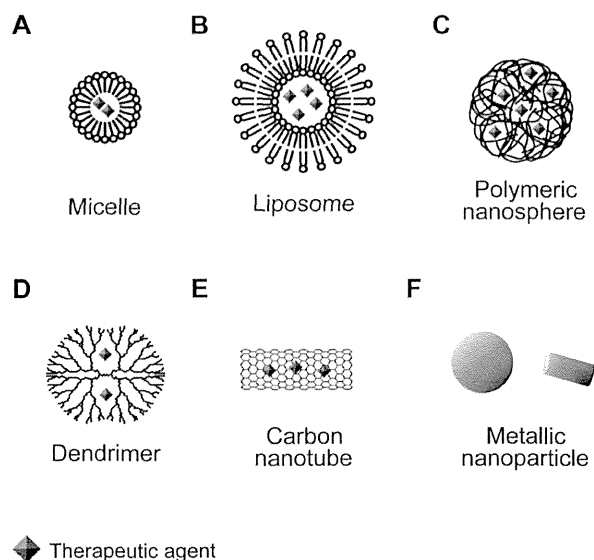   nanotube   nanoparticle

◆ Therapeutic agent

Figure 1. Schematic description of nanoparticle mediated drug delivery systems. **A:** Micelle self assembles from lipids or synthetic macromolecules with hydrophilic heads and hydrophobic tails in an aqueous solution. Placing hydrophobic tails inside, lipid micelles encapsulate hydrophobic therapeutic agents. **B:** Liposome is composed of lipid bilayer. Placing hydrophilic heads outside and inside, liposomes encapsulate hydrophilic solution and therapeutic agents inside. **C:** Polymeric nanosphere, formed from assembly of macromolecular polymers, contains hydrophilic and hydrophobic therapeutic agents. **D:** Dendrimer, composed of macromolecular polymer incorporating therapeutic agents within its structure. **E:** Carbon nanotubes, a cylindrical structure of covalently bonded carbon atoms, can carry therapeutic agent inside. **F:** Crystalline metals in nano-meter scale possess therapeutic or imaging function themselves.

cules with a controlled near monodisperse three-dimensional architecture emanating from a central core. Polymer growth starts from a central core molecule and growth occurs in an outward direction by a series of polymerization reactions, which determines the size of dendrimers starting from a few nanometers. Cavities in the core structure and folding of the branches create cages and channels for the incorporation of therapeutic agents (Figure 1D).[1,8] Carbon nanotubes belong to the family of fullerenes and consist of graphite sheets rolled up into a tubular form. The diameter and the length of single-walled nanotubes may vary between 0.5–3.0 nm and 20–1000 nm, respectively. Therapeutic agents are attached on either the inner or outer tube wall surfaces, which are the so-called filling or wrapping modes of binding, respectively (Figure 1E).[21] In contrast, metallic nanoparticles are functional themselves. Ion oxides are usually prepared as alkaline co-precipitation of Fe^{2+} and Fe^{3+} salts in water in the presence of a suitable hydrophilic polymer such as dextran or poly(ethyleneglycol). This yields an iron core of 4–5 nm in diameter, which is hexagonally shaped and surrounded by dextran or poly(ethyleneglycol) molecules to form superparamagnetic iron oxide particles (SPIO) (60-150 nm) as contrast agents for magnetic resonance imaging (MRI).[9,22,23] Gold nanoparticles possess the unique photodynamic properties of absorbing near-infrared light and emitting light and heat, and have been tested as a cancer photo-thermal therapy. Also, gold nanoparticles have been conjugated with various therapeutic agents and targeting moieties, and act as drug carriers (Figure 1F).[1]

Intravital kinetics of nano-DDS may be diverse; their behavior within the biological environment is affected not only by size, but also by their chemical makeup and morphology. However, the most important determinant of the physiological behaviors of nano-DDS is the size, as discussed below.

Physiological Behavior Of nano-DDS

Nano-sized materials (10–300 nm in diameter) tend to remain in circulation avoiding renal excretion, which is a primary feature of nano-DDS. While circulating in the blood stream, nano-DDS extravasates from the vasculature with enhanced permeability, such as angiogenic vessels in tumors, and vessels in organs after ischemia-reperfusion, which is an important mechanism that affects tissue distribution of nano-DDS.[2,5,24-26] The neovasculature in tumors lacks functional lymphatic vessels as well as enhanced vascular permeability, causing an accumulation of nano-DDS in the tumor microenvironment.[2] This phenomenon is referred to as enhanced permeability and retention (EPR) effects of nano-DDS.[27]

Recognition and incorporation by the mononuclear phagocyte system (MPS, also called the reticuloendothelial system), namely neutrophils, monocytes, and macrophages in the blood, liver, spleen, and lymph nodes is also a common physiological behavior for nano-DDS, which may affect the blood circulating time and tissue/cell distribution.[28-31] One of the first clinically approved nano-scale DDS therapies was a liposomal formulation of doxorubicin, a cytotoxic drug used for cancer chemotherapy. During its development, encapsulation of doxorubicin in liposomes prolonged its blood half-life compared to the free drug, but this was found to be unsatisfactory because of entrapment by MPS.[32] The addition of polyethylene glycol (PEG) to the surface of nano-DDS was shown to reduce the recognition of MPS, and in the case of doxorubicin liposomes, the addition of PEG reduced the clearance from the blood-stream, as well as cardiotoxicity, which is a major adverse effect.[32] On the other hand, incorporation into MPS itself is one of the mechanisms of drug delivery, especially when treating an inflammatory disease, such as atherosclerosis. Several studies employ this mechanism for the imaging and treatment of atherosclerosis, target-ing inflammatory monocytes/macrophages in atherosclerosis.[31]

The above-mentioned mechanisms underpin a 'passive-targeting' of nano-DDS on diseased organs or MPS. By contrast, an 'active-targeting' strategy employs a specific targeting structure on nano-DDS, which binds to the target molecule that is specific for a certain disease process. One good example is tumor-specific expression of folate receptor, which is targeted by addition of folate to the surface of nano-DDS.[33,34] For the treatment of cardiovascular disease, vascular endothelial cells can be targeted by an antibody for platelet endothelial cell adhesion molecule (PECAM-1). Liposomes loaded with a superoxide dismutase mimetic were conjugated with PECAM-1 antibody, which increased the delivery of liposomes to the pulmonary vasculature, and successfully enhanced the anti-inflammatory effects against endotoxin-induced acute lung injury.[35] Vascular cell adhesion molecule-1 (VCAM-1) is another molecule for targeting vascular endothelial cells.[36] There are still numerous opportunities for an 'active-targeting' strategy to find specific target molecules for a certain disease process, the effectiveness of which may be investigated in future studies.

Nano-DDS for Atherosclerosis

Atherosclerosis is one of the oldest diseases and was even present in ancient times, and atherosclerotic CVD, such as acute myocardial infarction (MI) and stroke, are still major causes of death and disability worldwide.[37] Atherogenesis begins as an endothelial dysfunction; when subjected to oxidative, hemodynamic, or biochemical stimuli (from smoking, hypertension, or dyslipidemia) and inflammatory factors, endothelial cells change their permeability and the expression of adhesion molecules to promote the recruitment of circulating monocytes and cholesterol-containing LDL particles. Inflammation and biochemical modifications ensue, causing endothelial and smooth-muscle cells to proliferate, produce extracellular matrix molecules, and form a fibrous cap over the developing atheromatous plaque.[38] Narrowing of the arteries by atheromatous plaque limits blood flow causing ischemic vascular diseases such as angina pectoris, whereas the rupture of a fibrous cap causes abrupt cessation of blood flow via thrombosis, resulting in end organ damage such as AMI. A series of pathological analyses in patients with sudden coronary deaths showed that ruptured coronary lesions typically have large necrotic cores and a disrupted fibrous cap infiltrated by macrophages with an expression of matrix metalloproteinases (MMP),[39,40] suggesting that inflammatory macrophages contribute to the destabilization and rupture of atherosclerotic plaques, resulting in a thrombotic occlusion of the coronary artery and AMI. Among the molecular and cellular mechanisms of long-term atherogenesis leading to plaque destabilization, (1) enhanced vascular permeability, (2) expression of adhesion molecules in endothelial cells, (3) accumulation of inflammatory monocytes (Ly6C^{high} CCR2$^+$ in mice, CD14^{high}CD16$^-$ in humans)/macrophages, and (4) expression of proteases that facilitates plaque destabilization are potential mechanisms for drug delivery, and thereby targets for imaging and therapeutic intervention of atherosclerotic cardiovascular disease including coronary artery disease.[13,23]

Computed tomography (CT) is a modality which has been extensively used for the imaging of coronary arteries in clinical practice. Recent advances in multi-detector CT that can simultaneously acquire a volume of images have enabled us to acquire a complete coronary angiogram in less than a minute. Iodine-containing contrast agents are used to image coronary arterial lumens, identifying the narrowing of coronary lumens by atherosclerotic lesions. Recent clinical studies also describe 'unstable plaque' by coronary CT, as defined by a luminal narrowing that is associated with expansive or positive vessel remodeling (PR), and low-attenuation plaques (LAP), which suggests a high risk for plaque rupture and acute coronary syndrome.[40,41] It is conceivable that imaging of plaque macrophages using nano-DDS is a more specific approach to identify high-risk unstable plaques. N1177 is a crystalline iodinated aroyloxy ester covered with a polymer, with a mean diameter of 259 nm.[42] N1177 is incorporated into cultured macrophages, raising the iodine content by approximately 100-fold compared with conventional CT contrast, and delivery to lesion macrophages was histologically confirmed in an atherosclerotic rabbit model. Finally, intravenous use of N1177 resulted in the detection of macrophage-rich arterial walls in animal models by CT,[42] and is being tested in clinical trials.[43]

MRI produces tomographic images with high soft-tissue contrast and spatial resolution, and is another important imaging modality for cardiovascular disease. SPIO are strong nanoscale contrast enhancers for MRI, and because of their remarkable biocompatible and biodegradable properties, several SPIO particles with diverse sizes, coatings, and targeting abilities have been applied for imaging of the inflammatory process of atherosclerosis and myocardial infarction.[22,23] Macrophages internalize SPIO, altering the local magnetic field and thus producing the T2 shortening effect as visualized by signal reduction. Monocrystalline iron oxide nanoparticles (MION)-47 have an approximate 5-nm diameter core of SPIO coated with an approximate 10-nm-thick dextran layer and have a long blood half-life, which facilitates their accumulation in macrophages of atherosclerotic plaques. Incorporation of MION-47 in macrophages in atherosclerotic lesions was confirmed histologically in a rabbit model. Increased Fe content causes loss in T2 signals, which enables negative imaging of macrophage-rich lesions.[44] Targeting VCAM-1 was also tested for the imaging of atherosclerotic lesions in a mouse model, and showed enhanced delivery of SPIO by VCAM-1 targeting.[36]

Our group has tested polymeric PLGA nanoparticles as a nano-DDS for the treatment of atherosclerotic plaque destabilization.[13] PLGA is a biodegradable material and is approved by the FDA and the European Medicine Agency for various DDS in human clinical use.[5,6] In atherosclerotic ApoE-deficient mice fed a high fat diet and infused with angiotensin II, neutrophils and monocytes in the peripheral blood and the aorta incorporated FITC-loaded PLGA nanoparticles (FITC-NP) 2 hours after injection, determined by flow cytometric (FCM) analysis (Figure 2A). FITC-NP accumulated in atherosclerotic lesions in the aortic arch (Figure 2B), and fluorescence microscopy analysis revealed that FITC signals are observed mainly in the macrophages of atherosclerotic plaques, which is partially blocked by depletion of monocytes by clodronate, suggesting that PLGA nanoparticles are delivered to atherosclerotic lesions partly through monocyte/macrophage phagocytosis, and directly via enhanced permeability in the lesions. Weekly intravenous treatment with PLGA nanoparticles containing the HMG-CoA reductase inhibitor pitavastatin reduced circulating inflammatory Ly6Chigh monocytes, macrophage infiltration to the atherosclerotic lesions in the aortic root, and plaque destabilization in the brachiocephalic arteries (Figure 2C, D).[13] Another group tested liposome-dependent delivery of siRNA against chemokine receptor CCR2, and showed successful delivery to spleen, bone marrow, and liver, and the inhibition of monocyte/macrophage recruitment to the aorta and atherosclerotic lesions.[31]

The above-mentioned studies consistently showed successful delivery of nano-DDSs including crystalline metal, polymers, and liposomes to monocytes/macrophages, mainly through physiological entrapment by MPS, and these nano-DDSs can be applied to both the imaging and treatment of atherosclerosis.

Nano-DDS for Acute Myocardial Infarction and Ischemia-Reperfusion Injury

Acute MI is a major cause of death and heart failure worldwide.[37,45,46] In patients with ST-segment elevation acute MI (STEMI), early reperfusion therapy is a standard strategy to limit MI size; however, recent cohort studies suggest that the
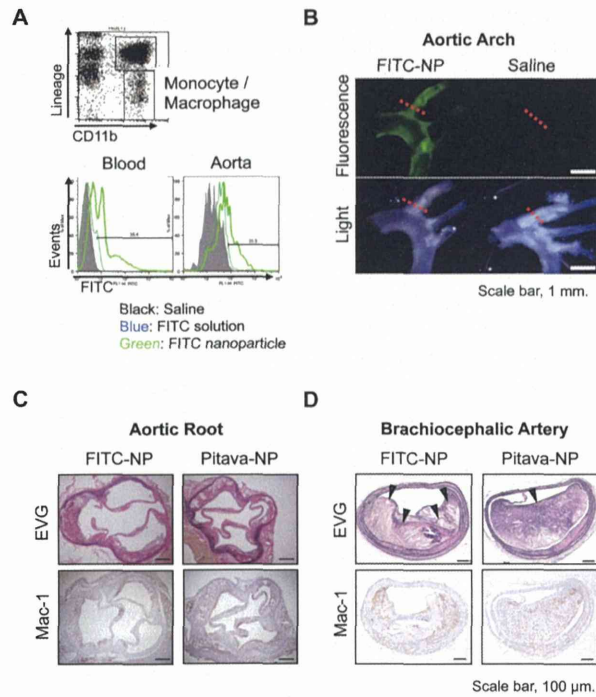
Figure 2. Nano-DDS for atherosclerosis. **A:** Flow cytometry of circulating leukocytes 2 hours after intravenous injection of PLGA nanoparticles encapsulated with FITC (FITC-NP). The histograms demonstrate FITC uptake by monocytes in the blood and the aorta. **B:** Fluorescent and light micrographs of isolated aortic arch 24 hours after intravenous injection of FITC-NP or saline. **C, D:** Photomicrographs of atherosclerotic plaques in aortic root (**C**) and brachiocephalic arteries (**D**) stained with EVG or Mac3. Arrows indicate disrupted/buried fibrous caps.

Figure 3. Nano-DDS for myocardial IR injury. **A:** Fluorescence reflectance imaging of the sections of heart in sham operated mouse or myocardial IR mouse. Accumulation of indocyanine green-loaded nanoparticle was noted in an IR heart after intravenous treatment at the time of reperfusion. **B:** Flow cytometric analysis in the leukocytes of an IR heart showed the incorporation of FITC-loaded nanoparticles was noted in macrophages and neutrophils.

mortality of MI patients has not improved despite significant reductions in door-to-balloon time in the last decade.[47] It is widely recognized that the reperfusion of coronary arteries paradoxically induces cardiomyocyte death, known as myocardial ischemia-reperfusion (IR) injury, for which several new therapeutic strategies are under investigation.[48,49] Myocardial IR induces the generation of reactive oxygen species (ROS), calcium overload, and rapid pH correction, all of which cause mitochondrial injury through the opening of the mitochondrial permeability transition pore (MPTP) and the activation of mitochondrial outer membrane permeabilization, leading to the necrosis and apoptosis of cardiomyocytes in the early phase (in several minutes) of IR injury. In the late phase of injury (over several hours), myocardial inflammation contributes to cardiomyocyte apoptosis and the healing of infarcted myocardium.[5,48,49]

The genetic ablation of cyclophilin D, a key regulatory molecule for MPTP opening, markedly reduces IR injury in mice.[50] In addition, intravenous administration of cyclosporine A (CsA), an inhibitor of cyclophilin D, at the time of reperfusion reduced myocardial IR injury in animals and in an early clinical trial in patients with acute MI.[51] The activation of pro-survival kinases, PI3K/Akt and Erk1/2 that are referred to as reperfusion injury salvage kinases (RISK), is another potential therapeutic target to attenuate reperfusion-induced necrosis and apoptosis and thus reduces MI size. Several pharmacological agents including statins and erythropoietin analogs have
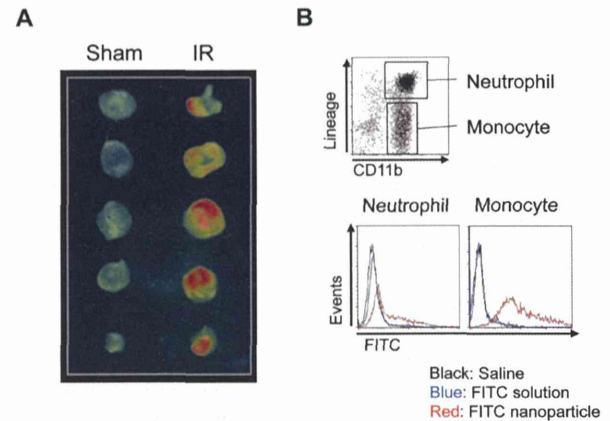
been shown to reduce MI size in animal studies. The recruitment of neutrophils and inflammatory monocytes is an established phenomenon after myocardial injury, and several animal studies have suggested a role of inflammation as a therapeutic target in IR injury.[31,49,52] However, several clinical trials on pharmacological cardioprotection for myocardial IR injury have failed to demonstrate a positive impact on clinical outcome in STEMI patients.[48,49] One possible explanation for the failure of current clinical trials is an insufficient drug delivery during a limited interventional time window, while administered at the time of reperfusion. Therefore, from a clinical perspective, it is feasible to apply an effective DDS that facilitates delivery to the sites of IR injury during reperfusion, a clinically feasible time point.

Nano-DDS may accumulate in injured tissues, including IR myocardium, where vascular permeability is enhanced.[5,24-26] Incorporation by circulating monocytes and other MPS is another mechanism targeting inflammation after myocardial injury.[31] Thus, nano-DDS may be feasible for myocardial IR injury targeting ischemic myocardium and inflammatory monocytes. Takahama, *et al* have tested PEGylated liposome-dependent delivery of adenosine during myocardial reperfusion, and found that liposomes attained a higher adenosine concentration in the ischemic myocardium and showed superior cardioprotection and less systemic hypotensive effect compared with free adenosine in a rat model.[26] Leuschner, *et al* have tested liposome-dependent delivery of siRNA against CCR2, and showed successful delivery to spleen, bone marrow, and liver, and the inhibition of monocyte/macrophage recruitment to the heart after IR. Treatment with siRNA-CCR2 successfully reduced MI size.[31]

We have examined the efficacy of PLGA nanoparticles as a DDS for myocardial IR injury. In a mouse model of myocardial 30-minute ischemia-reperfusion, PLGA containing indocyanine green-loaded PLGA nanoparticles was traced with fluorescence reflectance imaging. PLGA nanoparticles were found exclusively in the ischemic myocardium (Figure 3A). Flow cytometric analysis showed the incorporation of FITC-